Pertanika J. Sci. & Technol. 34 (4): 2023 - 2051 (2026)

PERTANIKA JOURNALS

SCIENCE & TECHNOLOGY

Journal homepage: http://www.pertanika.upm.edu.my/

Parametric Study of Reaction Parameter for Glycerol Acetylation and Reusability of Sulfated-Titania Catalyst

Shera Farisya Mohamad Rasid[1], Ernee Noryana Muhamad[1,2,3], Yun Hin Taufiq-Yap[1,2], Haizatul Izzatti Ridzuan[1], Siew Ling Lee[4,5], and Irmawati Ramli[1,2,3]*

[1]Department of Chemistry, Faculty of Science, Universiti Putra Malaysia, 43400 UPM Serdang, Selangor, Malaysia
[2]Catalysis Science and Technology Research Centre (PutraCAT), Faculty of Science, Universiti Putra Malaysia, 43400 UPM Serdang, Selangor, Malaysia
[3]Laboratory of Processing and Product Development, Institute of Plantation Studies, Universiti Putra Malaysia, 43400 UPM Serdang, Selangor, Malaysia
[4]Department of Chemistry, Faculty of Science, Universiti Teknologi Malaysia, 81310 UTM Johor Bahru, Johor, Malaysia
[5]Centre for Sustainable Nanomaterials, Ibnu Sina Institute for Scientific and Industrial Research, Universiti Teknologi Malaysia, 81310 UTM Johor Bahru, Johor, Malaysia

ABSTRACT

A parametric study of the reaction parameter for glycerol acetylation was conducted using a highly active sulfated-titania catalyst to determine the ideal conditions for achieving higher TA selectivity and glycerol conversion (GLC). The catalyst was prepared by impregnating titania with a 15% sulfuric acid solution, followed by calcination under CO_2 for 2 hours and denoted as the 15SA catalyst. The catalyst was subsequently analysed using TGA, XRD, BET, XPS, NH_3-TPD, and SEM-EDX. The characterisation results revealed that the 15SA catalyst possesses a sufficient surface area (1.9 m^2g^{-1}), a high density of acidic sites (342.6 $\mu molg^{-1}$) and good porosity. The study then examined the effects of several reaction parameters, including temperature (100 °C – 140 °C), molar ratio of glycerol (Gly) to acetic acid (Ac) (1:3 w/v – 1:15 w/v), catalyst loading (0.1 g – 0.9 g) and reaction time (1 h – 5 h). The catalyst was then reused for five successive cycles to evaluate its reusability. The results demonstrated that a higher density of acidic sites, sufficient BET surface area and pore volume of the catalyst may enhance the formation of GLC and TA in the glycerol acetylation by facilitating the diffusion of the glycerol molecules on the catalyst's surface.

ARTICLE INFO

Article history:
Received: 24 June 2025
Accepted: 19 June 2026
Published: 13 August 2026

DOI: https://doi.org/10.47836/pjst.34.4.04

E-mail addresses:
sherafarisya@gmail.com (Shera Farisya Mohamad Rasid)
ernee@upm.edu.my (Ernee Noryana Muhamad)
taufiq@upm.edu.my (Yun Hin Taufiq-Yap)
zatul9793@gmail.com (Haizatul Izzatti Ridzuan)
lsling@utm.my (Siew Ling Lee)
irmawati@upm.edu.my (Irmawati Ramli)
* Corresponding author

e-ISSN: 2231-8526

Therefore, optimal conditions for glycerol acetylation yielded a higher TA selectivity of 55 % and glycerol conversion of 97 % at a molar ratio of 1:6 w/v of Gly: Ac and a catalyst loading of 0.5 g at 130 °C for a 2 h reaction time. The reusability study showed that the 15SA catalyst can attain a higher GLC exceeding 97 % and a higher DA+TA selectivity of 85 % after five cycles. In contrast, the selectivity of TA reduced after five cycles due to the leaching of the acidic site from the catalyst, as proven by the EDX analysis.

Keywords: Acetins, acetylation, glycerol, parametric study, solid acid catalyst, sulfated-titania, triacetin

INTRODUCTION

The increasing population, rapid industrialisation, and growing energy have collectively precipitated an energy crisis associated with environmental deterioration, including ecological destruction, the scarcity of fossil fuels and pollution (Fauzi et al., 2025; Reinoso & Boldrini, 2020; Shikhaliyev et al., 2021). Therefore, utilising renewable energy as an alternative is essential for reducing environmental pollution while fostering social development and reducing reliance on conventional fossil fuels. Ladero (2021) stated that more than 280 billion US$ was invested worldwide in renewable energy from 2007 to 2017. These investments aim to attain a net-zero situation in greenhouse gas emissions (GHG). As a result, about 66 countries have committed to sourcing more than 50 % of their primary energy from renewable sources by 2050, including the Americas, Africa, the Asia-Pacific and the Indian Ocean (Dey et al., 2021). These developments have led to higher demand for biodiesel as a renewable transportation fuel, as it has been considered as one of the options to reduce consumption of fossil fuels and limit the generation of greenhouse gas emissions (Chilakamarry et al., 2021; Jose et al., 2023).

The transesterification of the biodiesel generates glycerol as a by-product. Hidayati et al. (2024a) and Malaika et al. (2023) stated that the production of glycerol increases linearly with biodiesel production. The ratio of glycerol to biodiesel is 1:10, yielding approximately 10 litres of glycerol for every 100 litres of biodiesel production (Reinoso & Boldrini, 2020). Therefore, excess production of glycerol has led to a significant price decline for several years and may become a challenge to the biodiesel industry since the unwanted glycerol cannot be disposed of in the environment (Mou et al., 2021; Shikhaliyev et al., 2021). Glycerol can be transformed into valuable chemicals with numerous applications, including in food, pharmaceutical, cosmetic, and plastic manufacturing. The low cost of glycerol has motivated researchers to valorise it via several processes, such as oxidation, transesterification, ammonization, condensation polymerisation, aromatisation, acetalisation, and acetylation reactions (Ebadi Pour et al., 2021; Hidayati et al., 2024b; Lee et al., 2026; Rathod et al., 2025; Singh & Gosu, 2025; Timofeeva et al., 2017). Among

these reactions, glycerol acetylation has gained significant attention because of its ability to yield three commercially important products: monoacetin (MA), diacetin (DA), and triacetin (TA).

The acetylation of glycerol with acetic anhydride or acetic acid involves a stepwise, consecutive reaction. In the first two reactions, MA and DA will form, followed by the formation of TA. All three products have useful industrial applications. For instance, MA is used in the production of explosives and smokeless powder, as a solvent in the leather tanning and dye industries and as a humectant in cosmetics (Beejapur et al., 2017; Kanimozhi et al., 2018). DA is used as a softening agent, building block in polyester, a solvent, a plasticiser, and an intermediate in the preparation of antidotes. (Appaturi et al., 2021; Beejapur et al., 2017; Kulkarni et al., 2020). TA is frequently used as an antiknock additive in petrol, an antimicrobial agent in pharmaceuticals and in cigarette filter production. In addition, the mixture of DA and TA can enhance the characteristics of petrodiesel. Kulkarni et al. (2020) stated that the incorporation of DA and TA can improve the properties of cold flow, viscosity, and biodiesel formulation quality. Furthermore, TA serves as a fuel additive by lowering the harmful emissions of unburned hydrocarbon (UHC), particulate matter (PM), nitrogen oxide (NOx), carbon monoxide (CO) and unregulated aldehyde (Jiang et al., 2019; Kalyani et al., 2023; Kulkarni et al., 2020; Ramos et al., 2025).

TA is the most valuable product in the acetylation of glycerol; however, its selectivity is usually lower than that of DA and MA. Therefore, various reaction conditions and catalysts have been investigated to improve TA formation. Some researchers have used acetic anhydride as the acetylating agent, achieving 100% TA selectivity at 60 °C within 20 min (Silva et al., 2010). Chandrakala et al. (2014) also obtained 100 % TA selectivity and 100 % GLC at 115 °C over a 30 min. Although acetylation of glycerol with acetic anhydride shows excellent performance in terms of TA selectivity and the GLC within a short period of time, acetic anhydride is more expensive, highly exothermic, and classified as a controlled substance in many countries due to its potential use as a precursor in narcotics production (Carpegiani et al., 2020; García-Martín et al., 2019; Mukhopadhyay et al., 2021; Okoye & Hameed, 2016; Okoye et al., 2017a). Therefore, acetic acid is preferred for the acetylation of glycerol as it is much cheaper and less toxic than acetic anhydride.

However, recent studies have shown that using acetic acid in glycerol acetylation without a catalyst has a low TA selectivity. For instance, Jiang et al. (2019) reported 0 % TA selectivity with 21 % GLC at 70 °C under atmospheric pressure. Similarly, Liu et al. (2019) obtained only 1 % TA selectivity with 48 % GLC at 125 °C over a 24 h reaction. Fauzi et al. (2025) achieved 0 % TA selectivity after testing at a reaction condition of 90 °C, 1:3 molar ratio of glycerol to acetic acid at 1 h reaction. Nonetheless, the GLC results were stated in their investigation of the blank reaction. Moreover, Kale et al. (2015) found that using 10 g glycerol and 39.16 g acetic acid at 105 °C for 4 h resulted in only 50 % of GLC and 0 % of TA selectivity.

The acid-catalysed mechanism has been widely used to facilitate the formation of TA and enhance GLC in the acetylation reaction. Heterogeneous catalysts, such as heteropolyacids, resins, zeolites, carbon catalysts and metal oxide catalysts, were widely employed compared to homogenous catalysts (Dalla Costa et al., 2017; Ferreira et al., 2009; Kulkarni et al., 2020; Magar et al., 2020; Nda-Umar et al., 2020a). The demand for heterogeneous catalysts in the acetylation process is increasing, as they can replace the liquid catalysts such as H_3PO_4, HCl, H_2SO_4, sulfonic acid, acidic ionic liquid, *para*-toluene, etc. Liquid catalysts have several drawbacks, including reactor corrosion, difficulty in separation, production of hazardous compounds, catalyst loss and poor catalyst reusability (Appaturi et al., 2021; Dalla Costa et al., 2017; Hidayati et al., 2024a; Karnjanakom et al., 2018; Khayoon et al., 2014). For instance, Ferreira et al. (2009) used dodecamolybdophosphoric acid encapsulated in USY zeolite (PMo1_NaUSY) as a heterogeneous acid catalyst for the glycerol acetylation with acetic acid and achieved 60 % GLC and a 4 % TA selectivity after 3 h of testing. Mou et al. (2021) attained 95 % GLC and 6 % TA selectivity by employing a 1:6 w/v molar ratio of Gly: Ac, 5.0 wt.% Amberlyst-15 catalyst, at a temperature of 90 °C for 1 h.

Moreover, Nda-Umar et al. (2020b) prepared a sulfonated carbon catalyst using a chemical method and subsequently conducted glycerol acetylation with a 1:6 w/v Gly: Ac molar ratio and a 0.5 g catalyst dosage for a reaction duration of 3 h. They found a remarkable catalytic activity with 56 % TA selectivity and 94 % GLC, attributed to the higher BET surface area and greater acidic capacity of the synthesised catalyst, as demonstrated by N_2 adsorption-desorption and NH_3-TPD analyses. Furthermore, Reddy et al. (2010) investigated the use of the metal oxides such as ZrO_2, TiO_2–ZrO_2, WOx/TiO_2–ZrO_2 and $MoOx/TiO_2$–ZrO_2 in glycerol acetylation with acetic acid, employing 1:6 w/v Gly:Ac molar ratio, 5 wt.% of catalyst dosage for 60 h reactions at 120 °C. They found that $MoOx/ TiO_2$–ZrO_2 achieved the highest GLC (~ 100 %) and TA selectivity (~80 %). Thus, it can be concluded that the carbon and metal oxide catalysts show an excellent performance in glycerol acetylation due to their high thermal stability, sufficient BET surface area and pore volume and good porosity, compared to zeolite, resin, and heteropolyacid catalysts. Nonetheless, the excessively long reaction time is unsuitable for industrial applications.

The synthesis of metal oxide catalysts for the acetylation of glycerol with acetic acid remains an active area of research to enhance TA selectivity. Testa et al. (2019) stated that the excellent catalytic performance in glycerol acetylation is related to the acid capability, strength and surface density of the acid sites of the catalyst. This is because the acetylation reaction can be catalysed not only by the Brønsted acid sites but also by Lewis acid sites (Fauzi et al., 2025). Therefore, incorporating the sulfate species onto the metal oxide catalysts could be an effective approach to increase the catalyst acidity and boost performance in glycerol acetylation.

Kulkarni et al. (2020) reported that the use of sulfated CeO_2-ZrO_2 catalyst resulted in a TA selectivity of 21 % due to high acid capacity (2.5 mmol), sufficient BET surface area (22 m^2g^{-1}) and good pore diameter (5.9 nm). In contrast, the non-sulfated CeO_2-ZrO_2 catalyst achieved only 0.5 % TA selectivity owing to its low acid site density. Moreover, Geetha et al. (2020) reported the same finding after examining the performance of sulfated-titania catalyst in a pseudo-five-component reaction. They found that the sulfate concentration of 5 wt.% in the preparation of sulfated titania via the sol gel method gave the highest yield (90 %) in the functionalization of piperidine, compared to non-sulfated titania (48 %) after a 30 min reaction under reflux conditions. The surface acidity of bare TiO_2 is 1600 µg, whereas the sulfated titania exhibits 2200 µg, as determined by the pyridine adsorption method. The sulfated-titania catalyst prepared via the sole gel method is also easily recyclable. Nevertheless, the sol-gel synthesis route requires precursor hydrolysis, which adds complexity to the preparation process.

The work conducted by Geetha et al. (2020) and Kulkarni et al. (2020) is similar to our previous study, which focused on the impact of the sulfuric acid concentration on the physicochemical characteristics of sulfated titania and evaluated its efficacy in GLC and acetin selectivity, particularly TA (Shera Farisya et al., 2021). We found that using sulfated TiO_2 with a 15 % concentration of sulfuric acid (15SA), prepared via the impregnation method, yielded a remarkable TA of 42 %, whereas non-sulfated titania exhibited only 16 % TA selectivity at 100 °C for a 2 h reaction. Despite its simple preparation, the 15SA catalyst demonstrated good catalytic performance owing to its high acid site density of 342.6 µmol g^{-1}, sufficient BET surface area of 1.9 m^2 g^{-1} and good porosity. However, the optimal reaction conditions for glycerol acetylation using 15SA catalyst were not determined in that study. Hence, the present work aims to further investigate the effect of reaction parameters, namely temperature, molar ratio of glycerol to acetic acid, catalyst loading and reaction time, on acetin selectivity, particularly TA selectivity and the GLC in glycerol acetylation over the 15SA catalyst using a systematic parametric approach. In addition, the reutilization of the 15SA sulphated titania catalyst was evaluated over five successive reaction cycles to determine its potential for repeated use in the catalytic reaction.

Materials

Sigma-Aldrich supplies acetonitrile (GC grade), 1,3-butanediol and titanium dioxide (98 %) while R&M chemicals provide sulfuric acid (95–98 %), glacial acetic acid (99 %) and anhydrous glycerol (99 %). No additional purification was required for any of the chemicals purchased.

Catalyst Preparation

The sulfated-titania catalyst was synthesised via the impregnation method as reported in our previous study (Shera Farisya et al., 2021). Briefly, about 15 % concentration of

the sulfuric acid was poured into 10 g of titanium dioxide. The sulfated-titania was then stirred for 24 h, filtered, and dried in an oven for 24 h at 100- 120 °C. Afterwards, the dried catalyst was ground, sieved (250 nm) and calcined for 2 h at a heating rate of 5 °Cmin $^{-1}$ under a CO_2 environment. Finally, the sulfated-titania catalyst was then stored in a tight bottle and denoted as 15SA.

Catalyst Characterisation

The thermal stability of the sulfated-titania catalyst was assessed using a Mettler Toledo 851e thermal analysis instrument. The crystalline phases of non-sulfated and sulfated-titania catalysts were evaluated using an X-ray diffractometer with a Shimadzu model XRD 6000. Cu Kα radiation source of 30 kW and electricity of 30 Ma was utilised, and the diffraction pattern was obtained within a scanning range of 2θ = 10–80° at a scanning speed of 4° min^{-1} using a wavelength (λ) of 1.54. The textural properties of the synthesised catalysts were determined using the nitrogen physisorption method with a Micrometrics analyser. Before the determination, the sample was degassed for 8 h at 120 °C to remove adsorbed molecules from the pores. To confirm the existence of the surface functional groups in the sulphated-titania catalyst, X-ray photoelectron spectroscopy (XPS) analysis was carried out using a PHI Quantera II instrument equipped with a monochromatic Al Kα X-ray source (photon energy, hv =1486.6 eV). The analysis was operated at 25.6 W, and data acquisition was performed using a pressure chamber below 10^{-8} mbar equipped with a charge neutralisation system. The Smartsoft-XPS and MULTIPAK ECSA software were employed to deconvolute the acquired data into multiple peak and the charging effect caused by surface contamination of the analysed sample was corrected using the carbon binding energy scale (C 1s peak). A Thermo Finnigan TPDRO series of NH_3-TPD coupled with a thermal conductivity detector (TCD) was employed to determine total acid density and the distribution of acid sites of the synthesised catalysts. The surface morphology and elemental components of the sulfated-titania catalyst were determined via SEM JEOL, JSM6400 Scanning Electron Microscopy attached with Energy Dispersive X-ray Spectroscopy (SEM-EDX). The conditions of TGA, XRD, BET, NH_3-TPD and SEM-EDX analysis were outlined in the supplementary data (S1).

Catalytic Test in the Acetylation of Glycerol

Parametric study of reaction parameter for glycerol over sulfated-titania catalyst (15SA) was investigated in this study, as shown in Figure 1. Briefly, about 0.5 g of 15SA catalyst and a 1:6 w/v molar ratio Gly: Ac (5 g of glycerol and 18.6 ml of acetic acid) were introduced into a 250 ml round-bottom flask. The detailed calculation for the molar ratio of glycerol to acetic acid is provided in supplementary data (S2). A reflux condenser was attached to the flask, which was then immersed in a silicone oil bath. Before starting the reaction, the

magnetic rod was added to the mixture. The reaction was conducted at 100 °C for 2 h of reaction time and then stirred at 450 rpm under reflux conditions. The product was then cooled and centrifuged at 3000 rpm for 10 min following the completion of the reaction. The GLC, MA, DA and TA components were further analysed using GC-FID (Agilent 7890A, FID, DB Wax 30 m x 0.25 mm ID x 0.25 µm). Approximately 1 µL of the final sample was injected into the GC-FID instrument, which was initially set at a temperature of 80 °C for 30 min. The temperature was then increased to 260 °C at a temperature ramping of 10 °C min^{-1} and then to 300 °C with a temperature ramping of 30 °C min^{-1}. The total analysis time was 22.3 min with He serving as the carrier gas at a rate of 1.3 mL min^{-1}. The detailed procedure for GC-FID, the equation for glycerol conversion and the selectivity of acetins are outlined in the supplementary data (S3).

Furthermore, to examine the influence of reaction temperature in the glycerol acetylation, the method was performed at varying temperatures of 110 °C, 120 °C, 130 °C and 140 °C while maintaining constant other parameters. The temperature yielding the highest TA was chosen for further investigation on the effect of the molar ratios of Gly: Ac (1:3 w/v, 1:6 w/v, 1:9 w/v, 1:12 w/v and 1:15 w/v), catalyst loading (0.1 g, 0.3 g, 0.5 g, 0.7 g and 0.9 g) and reaction durations (1 h, 2 h, 3 h, 4 h and 5 h) to determine the parametric study for glycerol acetylation over the 15SA catalyst using one-factor-at-one time (OFAT). Finally, the reusability of the 15SA catalyst was evaluated at the ideal glycerol acetylation conditions, as shown in Figure 2. After completing each cycle, the spent catalyst underwent centrifugation, filtration and multiple washes with acetone to eliminate organic impurities. The catalyst was subsequently placed in an oven at 100 – 120 °C for a duration of 2 h. The catalyst was used up to the fifth cycle, and the leaching of the active site was determined using EDX analysis.

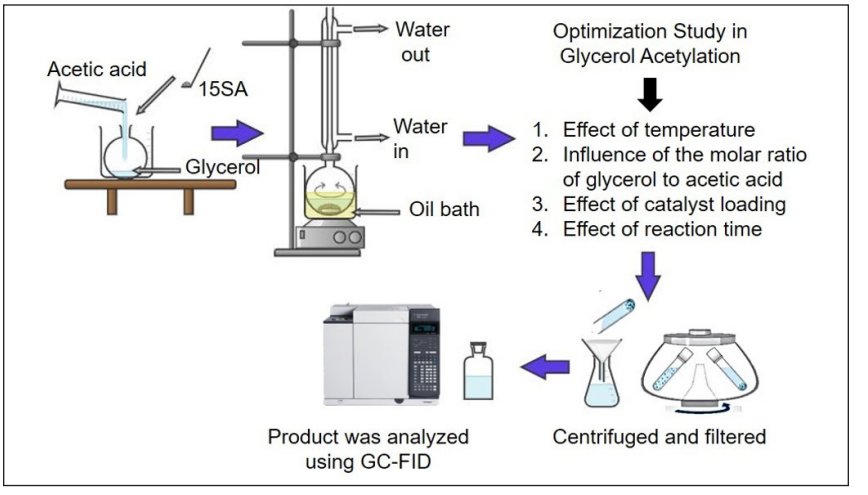

Figure 1. Experimental setup for acetylation of glycerol with acetic acid using a reflux condenser

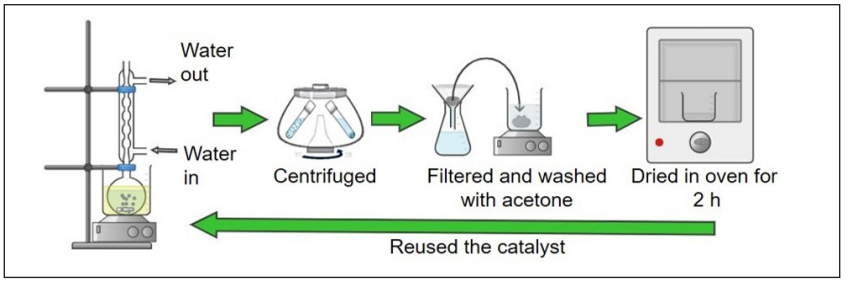

Figure 2. The procedure for the reusability study with the 15SA catalyst

RESULTS AND DISCUSSIONS

Physicochemical Properties of the Sulfated Titania Catalyst

15SA catalyst was characterised using X-ray diffractometer (XRD), Brunauer-Emmett-Teller (BET), X-ray photoelectron spectroscopy (XPS), Temperature-programmed desorption with ammonia (NH_3-TPD) and Scanning electron microscopy with Energy Dispersive X-ray (SEM-EDX). Thus, in this current study, the 15SA catalyst was further used for optimising the TA and GLC. Finally, the reusability of the catalyst was identified at optimal reaction conditions.

Crystallinity and Phase Determination Using XRD

Figure 3 illustrates the X-ray diffraction patterns for 15SA sulfated-titania catalysts. It was found that the 15SA catalyst exhibits anatase and $(TiO)(SO_4)(H_2O)$ peaks. The anatase peaks were detected at $2\theta = 38.64°$, 53.92°, 62.22°, 62.74° and 75.12° (JCPDS-ICDD card: 96-900-8214). According to the X'pert High Score Plus Software, the anatase peak has a tetragonal structure with a chemical formula of Ti_4O_8. In addition, the peaks detected at $2\theta = 25.34°$, 36.94°, 37.78°, 55.08°, 68.68°, 70.29°, 76.14° correspond to the $(TiO)(SO_4)(H_2O)$ peak with an orthorhombic structure (JCPDS-ICDD card: 96-153-0152). Therefore, the detection of $(TiO)(SO_4)(H_2O)$ peaks in the 15SA confirmed that the sulfate species are well distributed on the surface of the catalyst. Besides, Wijaya et al. (2021) and Yang et al. (2019) discovered that the sulfation of the catalyst leads to dissolution of the titania and reduces the peak intensity as compared to that of the untreated titania catalyst. This phenomenon promotes the generation of Ti-O-S and thereby renders the phase more amorphous (Pratika et al., 2021). As a result, a lower crystallinity of the $(TiO)(SO_4)(H_2O)$ with 39.27 nm was found at the peak of 25.3 °, whereas TiO_2 anatase exhibit crystallite size of 54.02 nm as calculated using the Debye-Scherrer formula. Furthermore, X'Pert High Score Plus software shows that the average particle size of 15SA is smaller than that of TiO_2 anatase with 36 nm and 80 nm, respectively. Jenie et al. (2010) and Parida et al. (2008) reported that the impregnation of the titania surface with sulfation is facilitated by the different molecular

size of sulfate ions (0.242 nm) and TiO_2 (220 nm). This impregnation inhibits the phase transformation from anatase to rutile, resulting in smaller crystallites of sulfated titania.

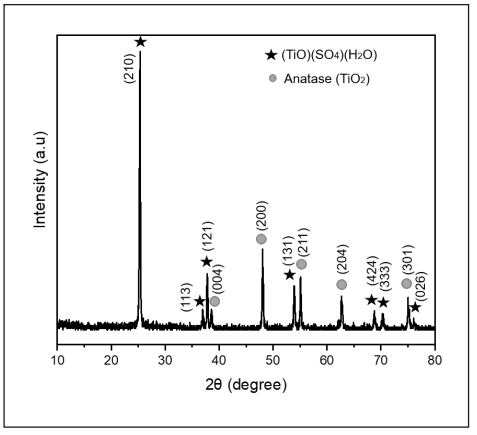

Figure 3. XRD profile for 15SA catalyst

Thermal Stability Determination Using TGA-DTG Analysis

The thermal stability and decomposition of the 15SA catalyst were investigated using the TGA analysis with a constant supply of N_2 gas at 50 $mLmin^{-1}$. Figure 4 illustrates three distinct stages of weight loss that were detected following thermal analysis. The initial decomposition began at the onset of the heating process, reaching 200 °C. This decomposition is attributed to the removal of water from the surface of the catalyst. The weight loss in this lower temperature region was about 2 ± 0.5 %. The subsequent decomposition was observed in a temperature range of 450 °C to 700 °C with a weight loss of 11± 0.5 %. This stage was associated with the decomposition of sulfate species. This finding agrees with the work reported by Noda et al. (2003), indicating that the decomposition between 450 °C and 700 °C was attributable to the sulfate bound to the oxide. Additionally, a less pronounced peak with a weight loss of 2 ± 0.5 % was detected between 800 °C and 950 °C in the DTG. This indicates that a high concentration of sulfuric acid (15 %) impregnated with titania requires more heat to break the intermolecular bond of the sulfate. Thus, at a higher temperature, SO_4^{2-} in the sulfated sample will escape as SO_2. This finding is correlated with Enríquez et al. (2013) and Liu et al. (2020).

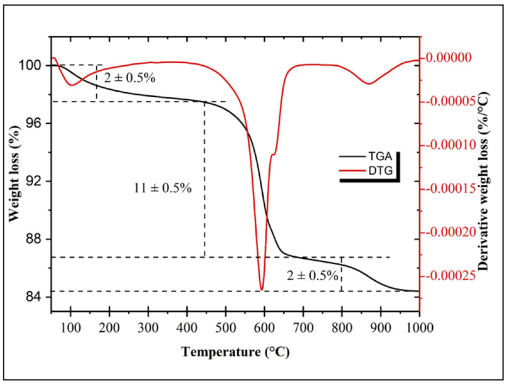

Figure 4. TGA-DTG profile for 15SA catalyst

Surface Area and Pore Size Distribution

Table 1 illustrates the BET surface area, BJH pore volume and pore size of the sulfated-titania (15SA) and non-sulfated-titania (TiO_2). The BET surface area of TiO_2 and 15SA decreased from 11.8 m^2g^{-1} to 1.9 m^2g^{-1} after the incorporation of SO_4^{2-} into the titania. This reduction might be due to the plugging of the pores and surface coverage by sulfate species (Lertna et al., 2022). This finding is consistent with work reported by Tomer and Biswas (2020),

which demonstrated that the sulfation of TiO_2 results in a lower BET surface area. A similar trend of BET surface area is observed in the pore volume, which decreases from 0.0029 cm^3g^{-1} for TiO_2 to 0.00003 cm^3g^{-1} for 15SA. Pore blockage could have occurred due to the increasing of the atomic radius of the sulfated-titania catalyst due to the replacement of one atom in the O-Ti-O framework by SO_4^{2-} ion after impregnation on TiO_2 (Tomer & Biswas, 2020). This observation was aligned with Zhou et al. (2015), who reported that agglomeration on the nano-sized $Ti(SO_4)$ occurred as more sulfate species were loaded on the surface, hence diminishing the surface area and porosity of the catalyst. Meanwhile, the pore diameter remains relatively constant for both catalysts, obtaining 5.2 nm for 15SA and 5.4 nm for non-sulfated TiO_2. This finding suggests that sulfation does not change the intrinsic structure of the pores but increases the deposition of sulfate groups, which might enhance the acidity of the sulfated catalysts. Additionally, both 15SA and TiO_2 catalysts can accommodate the glycerol molecule (1 nm) for the reaction to occur on the pore surface, thereby potentially enhancing the conversion of glycerol in glycerol acetylation with acetic acid.

Table 1
BET surface area, BJH pore volume and pore diameter for sulfated and non-sulfated catalysts

Catalyst	BET Surface Area (m^2g^{-1})	BJH Pore Volume (cm^3g^{-1})	Pore Diameter (nm)
TiO_2	11.8	0.0029	5.4
15SA	1.9	0.0003	5.2

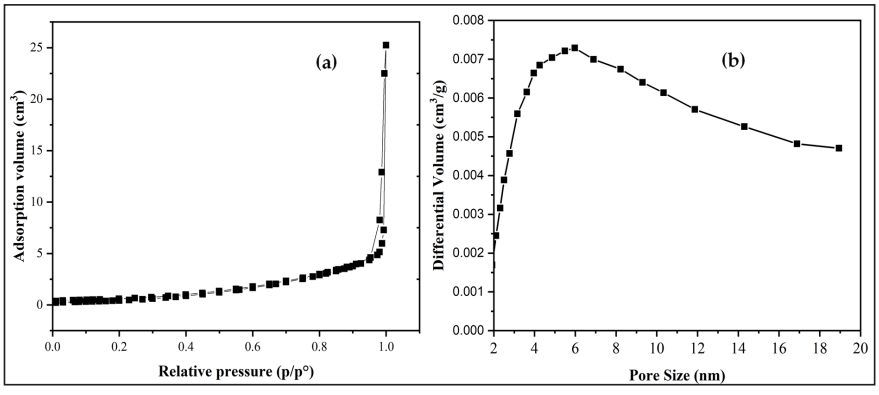

Figure 5. (a) N_2 adsorption- desorption isotherms (b) and pore size distribution of 15SA catalyst

Figure 5 reveals that the nitrogen adsorption-desorption isotherm of the sulfated catalyst is categorised as type IV, exhibiting a sharp descent at a relative pressure of 0.9-1.0 p/p°. These findings confirm that the 15SA catalyst exhibits a regular mesoporous structure. These results align with those of Afshar et al. (2015), Huang et al. (2017), and Tomer and Biswas

(2020). Moreover, according to the IUPAC classification, 15SA catalysts have prominent H1-type hysteresis loops due to variations in absorption and desorption. Furthermore, the pore size distribution, which ranges from 2 to 20 nm, provided additional evidence for the mesoporous nature of 15SA.

Surface Analysis Using XPS

The high-resolution XPS spectra scan of the 15SA catalyst is displayed in Figure 6. From this analysis, the oxidation state of sulfur and the bonding characteristic of the sulfated catalyst can be determined. Three intense XPS peaks were observed at binding energies of 458 eV, 531 eV and 169 eV, which are assigned to Ti 2p, O 1s, and S 2p, respectively, as illustrated in Figure 6a. In addition, Figure 6b revealed that the Ti 2p XPS spectra exhibit two significant peaks corresponding to Ti $2p_{3/2}$ and Ti $2p_{1/2}$ at 459.6 eV and 465.3 eV, respectively. These characteristic peaks confirm the presence of the anatase phase of titania, consistent with findings from the XRD. In addition, the Ti in 15SA is mainly present in the Ti^{4+} chemical state with a spin-orbital splitting value of 5.7 eV (Shi & Li, 2014; Tomer & Biswas, 2020).

Figure 6c shows the O 1s spectra, which can be deconvoluted into three distinct peaks. The lower bonding energy peak at 530.8 eV is associated with the Ti-O-S bonds, indicating the integration of sulfate groups into the titania framework. Meanwhile, the O-S bonds in the sulfate groups were observed at the elevated peak of 532.5 eV

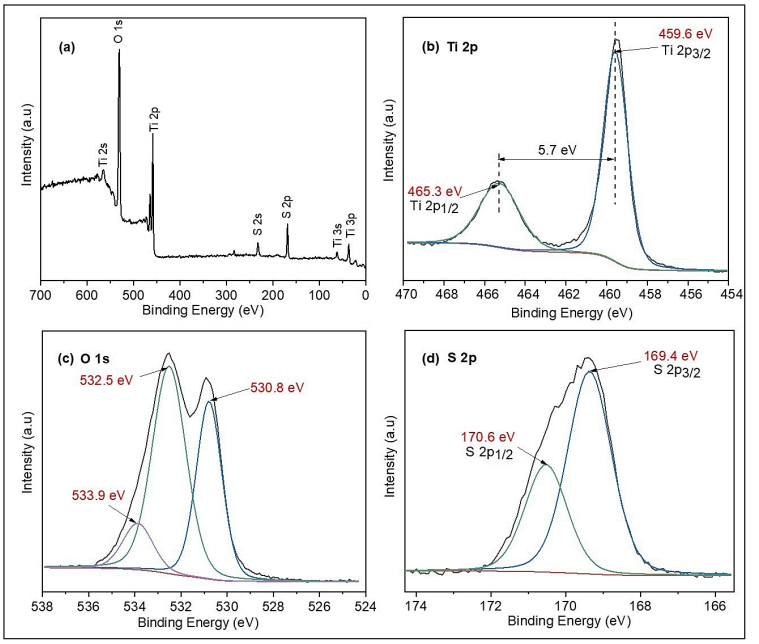

Figure 6. (a) Survey scan XPS spectra, (b) Ti 2p, (c) O 1s, and (d) S 2p of 15SA catalyst

(Dabbawala et al., 2018; Gardy et al., 2016; Tomer & Biswas, 2020). Additionally, the minor peak at 533.9 eV is associated with the O-H bond from the chemically bound water molecules on the catalyst surface (Patil et al., 2019; Zhao et al., 2014). In Figure 6d, the S 2p spectra are depicted with two deconvoluted peaks at photoelectron binding energies of 170.6 eV and 169.4 eV, which correspond to S $2p_{1/2}$ and S $2p_{3/2,}$ respectively. These peaks confirm the existence of SO_4^{2-} species on the surface of the 15SA catalyst. Similar peak assignments at comparable binding energies for sulfate groups have been reported in studies on sulfated metal oxides (Dabbawala et al., 2018; Shi & Li, 2014; Tomer & Biswas, 2020).

Analysis of Total Acid Sites Density Using NH_3-TPD

Ammonia-Temperature Programmed Desorption (NH_3-TPD) analysis was utilised to measure the comprehensive acid strength of the synthesised catalyst (Azri et al., 2021; Kanimozhi et al., 2018). The NH_3−TPD profile for the 15SA catalyst is displayed in Figure 7. Wang et al. (2015) and Yang et al. (2019) mentioned that the acid strength of the surfaces is theoretically correlated with the NH_3 desorption temperature. The desorption peaks at lower temperatures correspond to the physically bound NH_3, while the peaks at higher temperatures indicate chemically bound NH_3 (Dantas et al., 2017). The adsorption of NH_3 is correlated with the interaction force between ammonia and acidic sites, which are categorised into weak acid sites (T_{max} =10-250 °C), moderate acid sites (T_{max} = 250-500 °C), and strong acid sites (T_{max}>500 °C) (Azri et al., 2021; Srivastava et al., 2017). In addition, Figure 7 shows that the maximum desorption peak for the 15SA catalyst was found at 608 °C, with a total amount of adsorbed ammonia of 342.6 μmolg^{-1}. This result proves that the 15SA catalyst only exhibits a strong acid site density as the maximal desorption temperature is recorded at a temperature exceeding 500 °C. This finding aligns with the TGA-DTG profile, which indicates that the loss of sulfate species occurred within a temperature range of 450 °C to 900 °C. Furthermore, a larger desorption temperature of the 15SA catalyst suggests that the number of available active sites is higher, thereby increasing the acidic strength, regardless of Brønsted and Lewis acidity (Neto et al., 2020; Pratika et al., 2023). According to the Lewis theory, the NH_3 donates a pair of electrons and attaches to the Lewis acid centre (Ti^+) to form a covalent bond, while the Brønsted-Lowry theory indicates that NH_3 acts as a base by accepting a proton (H^+) from the Ti-OH molecules and forming an ammonium ion (NH_4^+) (Hu et al., 2015; Ropero-Vega et al., 2010). As a result, the sulfate species at 15SA are strongly bound to the titania surface, resulting in a higher total amount of adsorbed ammonia as displayed in Figure 7. Therefore, the presence of a higher acidic sites, strong acidic strength, sufficient pore volume and BET surface area in the catalyst, proven by NH_3-TPD, TGA-DTG and BET analyses, potentially enhanced the GLC and TA formation in the glycerol acetylation by facilitating the diffusion of the glycerol molecules on the catalyst's surface.

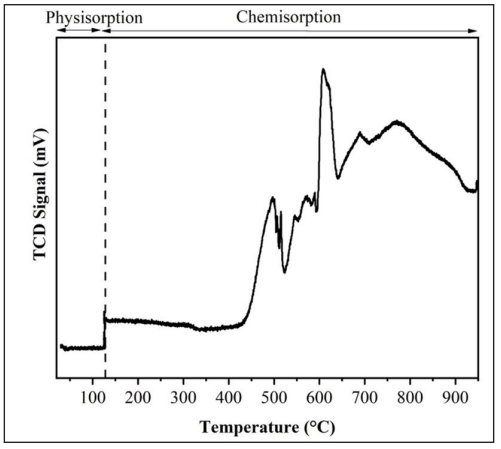

Figure 7. NH_3-TPD profile for 15SA catalyst

Scanning Electron Microscopy - Energy Dispersive X-Ray (SEM-EDX) Analysis

The element composition and the surface structure of the 15SA catalyst were analysed using SEM-EDX analysis. According to SEM analysis, the spherical particles with a crumb-like structure were found to be agglomerated, as shown in Figure 8, with an average size of 1 µm (from the scale bar). These findings align with the BET analysis, which indicates that the incorporation of a higher concentration of sulfuric acid on the titania surface leads to the blockage of the sulfate species, thereby resulting in a lower BET surface area. Tomer and Biswas (2020) also reported the same finding, where the agglomeration of particles resulted from the electrostatic interaction between the sulfate ions on the surface of the sulfated-titania catalyst. Furthermore, the EDX analysis indicates that the peaks of 15SA were detected at 0.5 keV, 0.6 keV, 2.3 keV, and 0.4 keV, respectively. This indicates that the 15SA catalyst is composed of titania (Ti), oxygen (O), and sulfur (S) in proportions of 33 %, 56 %, and 6 %, respectively. Therefore, the detection of S in this analysis confirms that the sulfation was successfully carried out.

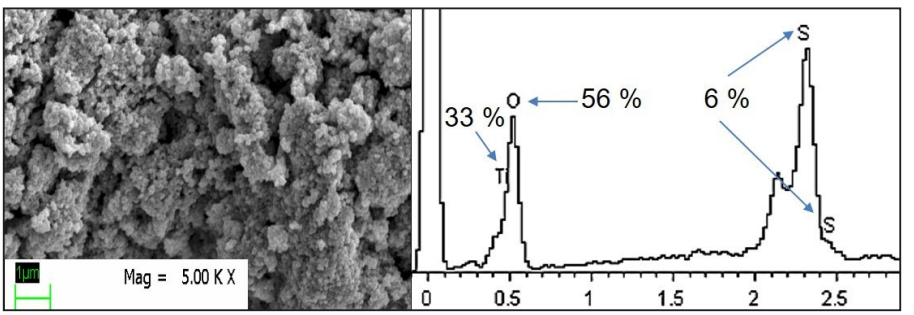

Figure 8. SEM micrograph for fresh 15SA catalyst

Systematic Investigation on the Effect of Temperature in Glycerol Acetylation

A series of reactions was conducted at temperatures ranging from 100 °C to 140 ° to examine the impact of reaction temperature (T) on GLC and the formation of acetins, particularly TA. The tests were carried out using a fixed 0.5 g dosage of the catalyst (CL) and a molar ratio of 1:6 w/v Gly: Ac (MR) for a reaction duration (t) of 2 h. According to Figure 9, the GLC remained consistently high (98±1 %) between 100 °C and 120 °C. These results

may be attributed to the near-complete consumption of glycerol, the limiting agent, under the excess acetic acid conditions imposed by the 1:6 w/v molar ratio, whereby surplus acetic acid cannot be completely utilised in the reaction (Hidayati et al., 2024a). However, the GLC marginally decreased from 97 % and 92 % when the temperature was raised to 130 °C and 140 °C, respectively. This reduction is consistent with the partial evaporation of acetic acid (boiling point: 118 °C, which reduces the effective concentration of acetic acid available under reflux conditions, rather than indicating any loss of catalyst activity (Hidayati et al., 2024a; Mufrodi et al., 2014). Overall, the GLC remained high across all tested conditions, exceeding 97 % except at 140 °C, where more acetic acid transforms into vapour within the 2 h reaction period, as observed by Kanimozi et al., (2018).

Moreover, Figure 9 shows that MA selectivity declined from 9 % to 5 % as the temperature increased from 100 °C to 130 °C, while DA selectivity followed the same trend, decreasing from 49 % at 100 °C to 41 % at 130 °C. In contrast, TA selectivity increased progressively from 42 % at 100 °C to a maximum of 55 % at 130 °C. This observation is consistent with the findings of Malaika et al. (2021), who reported that DA and TA are the dominant products at higher temperatures, while MA prevails at lower temperatures. This trend reflects the endothermic and thermodynamically controlled nature of the sequential acetylation pathway from MA to DA to TA. As reported by Okoye et al. (2017b), glycerol acetylation involves three consecutive reaction steps in which MA form first, followed by DA and TA, and the reaction is also highly dependent on temperature owing to its endothermic character. Each subsequent acetylation step required progressively more activation energy, and the third step (DA → TA) is the most thermodynamically demanding. At 130 °C, the 15SA catalyst, which possesses exclusively strong acid sites as evidenced by NH_3-TPD (T_{max} = 608 °C, total acidity = 342.6 μmol g^{-1}), provides a thermally compatible environment where the elevated temperature supplies sufficient energy to surmount the activation barrier for TA formation, while the active SO_4^{2-} species remain thermally stable well below their decomposition onset at 450 °C, as confirmed by TGA analysis. Furthermore, based on the Arrhenius equation, a higher reaction temperature results in a lower activation energy required for the conversion of reactant to products, increasing the rate constant. The higher frequency of molecular collisions at elevated temperature promotes better interaction between the reactant molecules and the strong Lewis (Ti^{4+}) and Brønsted (Ti-OH) acid sites of 15SA, thereby enhancing the formation of DA and TA (Appaturi et al., 2023).

However, a further increase in temperature to 140 °C resulted in a decline in TA selectivity to 38 % and DA selectivity to 48 %, as shown in Figure 9. This observation is attributed to the reduced availability of acetic acid due to its volatilisation at this temperature, which limits the progression of the reaction towards TA formation (Hidayati et al., 2024a). Therefore, it can be concluded that the 130 °C optimum represents a

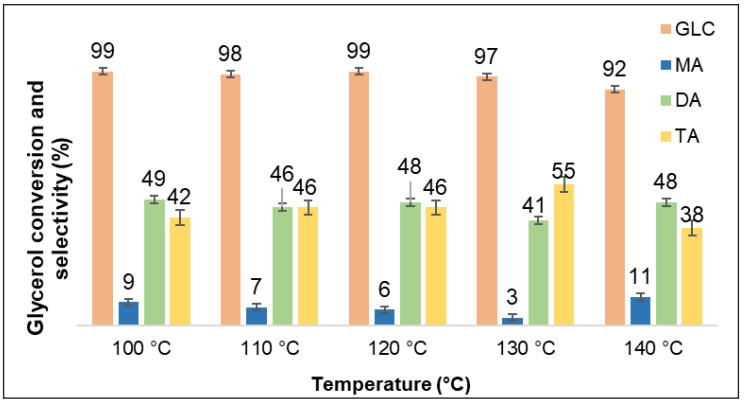

Figure 9. The effect of temperature (T) on the GLC and acetins selectivity. (Reaction condition: MR = 1:6 w/v glycerol: acetic acid, CL = 0.5 g, t = 2 h, T = 100-140 °C)

kinetic-thermodynamic balance specific to this catalyst system: sufficiently high to drive the endothermic DA to TA step at a competitive rate, yet below the threshold at which reagent depletion becomes significant. Despite the slight reduction in the GLC from 98 % at 120 °C to 97 % at 130 °C, the main objective of this study is to achieve higher TA selectivity. Thus, 130 °C was selected as the optimal reaction temperature, as it yields the highest TA selectivity of 55 %.

Influence of Molar Ratio of Glycerol to Acetic Acid in Glycerol Acetylation

The influence of the glycerol to acetic acid molar ratio on GLC and acetin selectivity is shown in Figure 10. In this study, the Gly: Ac molar ratio was varied at 1:3 w/v, 1:6 w/v, 1:9 w/v, 1:12 w/v and 1:15 w/v, while the other conditions were fixed at 130 °C, 0.5 g catalyst dosage for 2 h of reaction time.

Figure 10 shows that increasing the Gly: Ac molar ratio from 1:3 w/v to 1:15 w/v resulted in excellent glycerol conversion exceeding 90 % under all conditions, confirming that acetic acid availability does not limit GLC in these experiments. The shift in product selectivity is best explained by the stoichiometry of the stepwise acetylation reaction and the surface chemistry of the 15SA catalyst. At the 1:3 w/v molar ratio, only three moles of acetic acid are available per mole of glycerol, representing the theoretical minimum for full conversion to TA. However, the absence of excess acetic acid means the equilibria cannot be effectively driven forward, and MA remains the dominant product at 24 % selectivity, as only the first acetylation step can be completed before acetic acid is consumed. This observation aligns with the findings of Appaturi et al. (2021), who reported that a limited amount of acetic acid at a 1:3 w/v molar ratio restricts reagent availability in glycerol acetylation, favouring the formation of the mono-substituted product, MA.

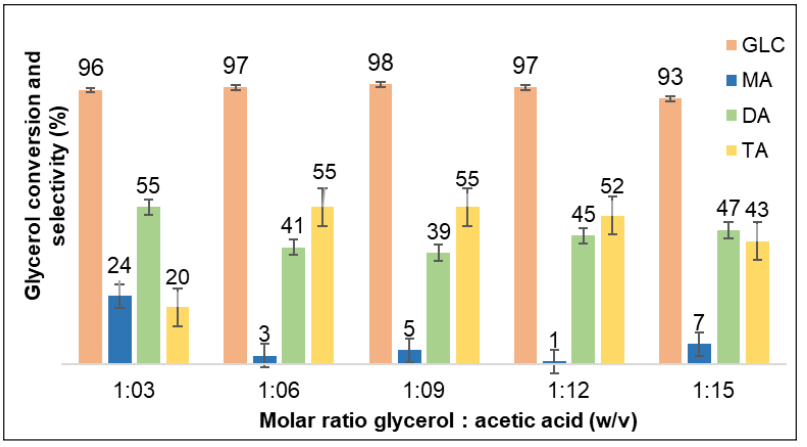

Figure 10. The effect of molar ratio of glycerol to acetic acid (MR) on the GLC and acetins selectivity. (Reaction condition: MR = 1:3-1:15 w/v Gly:Ac, CL = 0.5 g, t = 2 h, T = 130 °C)

TA selectivity increased significantly from 20 % to 55 % as the Gly: Ac molar ratio was raised from 1:3 w/v to 1:6 w/v. Increasing the ratio to 1:6 w/v creates a two-fold excess of acetic acid on the 15SA surface. First, it ensures that the Brønsted acid sites (Ti–OH), confirmed by the O 1s XPS peak at 533.9 eV, continuously protonate acetic acid molecules to generate acylium ions, sustaining the forward reaction. Second, the higher acetic acid concentration reduces the interfacial viscosity of the reaction mixture as reported by Fronza et al. (2025), improving mass transfer to reactants to the mesoporous catalyst surface. The 5.2 nm pore diameter of 15SA accommodates glycerol molecules (~1 nm) within the pore channels, enabling repeated sequential encounters with active sites and promoting the full MA to DA TO ta cascade. Acetic acid may also act as a Brønsted acid to further drive the forward reaction and enhance TA formation (Abida et al., 2020; da Silva et al., 2020). These effects explain why TA selectivity peaks at 55 % under the 1:6 w/v molar ratio.

GLC and TA selectivity declined slightly when the molar ratio was further increased to 1:12 w/v and 1:15 w/v, yielding 97 % GLC with 52 % TA selectivity at 1:12 w/v, and 93 % GLC with 43 % TA selectivity at 1:15 w/v. For the 15SA catalyst, excess acetic acid beyond 1:9 w/v is proposed to compete with glycerol intermediates for the limited number of strong Lewis's acid sites (Ti^{4+} centres), absorbing non-productively and occupying sites that would otherwise catalyse the final DA → TA acetylation step. This interpretation is consistent with the relatively low BET surface area of 15SA (1.9 $m^2\ g^{-1}$), which limits the number of accessible active sites. A large excess of acetic acid, therefore, disproportionately competes for these sites, as similarly reported by Okoye et al. (2017b), who found that excess acetic acid in the catalytic reaction led to a lower TA formation, likely due to mass transfer resistance limiting contact between glycerol and the catalyst surface. Therefore, the optimal Gly: Ac molar ratio was achieved at 1:6 w/v, representing the best balance

between reagent driving force and active site accessibility on the 15SA surface, yielding maximum TA selectivity of 55 % and GLC of 97%.

Effect of Catalyst Loading in Glycerol Acetylation

The effect of catalyst loading on the GLC and selectivity of MA, DA and TA was evaluated under fixed conditions: a molar ratio of 1:6 w/v Gly: Ac at 130 °C for 2 h. The catalyst loading was varied from 0.1 g to 0.9 g, and the results are presented in Figure 11.

As shown in Figure 11, glycerol conversion increased from 91 % to 98 % as the catalyst loading rose from 0.1 g to 0.3 g. The glycerol conversion showed no significant change when the catalyst loading rose to 0.5 g and 0.7 g, reaching 97 % for both, and slightly improved to 100 % at 0.9 g catalyst loading. This trend may be due to the increased availability of active sites, both Lewis (Ti^{4+}) or Brønsted (Ti–OH), as the catalyst dosage increases, which promotes higher glycerol conversion (Hidayati et al., 2024a).

In addition, TA selectivity increased from 38 % to 55 % as the catalyst dosage was raised from 0.1 g to 0.5 g, while MA selectivity declined from 11 % to 3 % over the same range. This response reveals a nuanced relationship between active site density and product distribution, specific to the strong-acid, low-surface-area character of the 15SA catalyst. At 0.1 g, the catalyst provides insufficient strong acid sites to drive the thermodynamically demanding DA to TA step at a competitive rate within 2 h window, resulting in DA (45 %) and MA (11%) dominating the product distribution. According to the mechanism reported by Spataru et al. (2021), the carbonyl group of acetic acid combines with the protons from the catalyst to form an acylium ion, which is then attacked by the hydroxyl groups of produce MA first, followed by DA and finally TA. As the loading increases to 0.5 g, the cumulative density of SO_4^{2-}–Ti^{4+} Lewis acid sites and Ti–OH Brønsted acid sites becomes sufficient to complete all three sequential acetylation steps within the reaction window. TA selectivity peaks at 55 % with 0,5 g, representing the threshold loading at which the strong acid site population is sufficient to drive the full MA to DA to TA cascade. Appaturi et al. (2021) similarly reported that the acetylation reaction over solid catalyst mainly occurs as a surface reaction, where active sites enhance the interaction between acylium ions and hydroxyl ions, facilitating the formation of higher DA and TA (Dhawan et al., 2021; Fronza et al., 2025; Shikhaliyev et al., 2021).

Moreover, Figure 11 shows that further increasing the catalyst dosage to 0.7 g and 0.9 g led to a slight decrease in TA selectivity to 43 % to 39 %, respectively, while MA and DA selectivities increased. At 0.7 g, MA selectivity increased to 10 % while DA selectivity rose to 45 %. At 0.9 g, MA and DA selectivities reached 10 % and 51 %, respectively. This decline in TA selectivity at loadings above 0.5 g is a consequence of poor bulk mixing rather than any reduction in intrinsic catalyst activity. Beyond 0.5 g, the increased solid mass creates a suspension too dense for efficient agitation at 450 rpm within the 250 ml

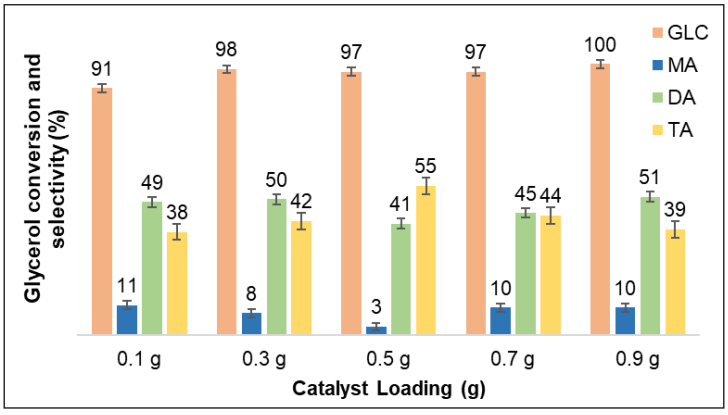

Figure 11. The effect catalyst loading (CL) on the GLC and acetins selectivity. (Reaction condition: MR= 1:6 w/v Gly:Ac, t = 2 h, T = 130 °C and CL = 0.1 - 0.9 g)

round-bottom flask used, increasing the inter-particle diffusion path length for glycerol and acylium intermediates and effectively confining reactions to the outer surfaces of catalyst agglomerates. This suppresses the final DA → TA step, which requires the most intensive substrate-surface contact, and is consistent with the SEM observations showing agglomeration in suspension. A similar observation was reported by Appaturi et al. (2021), who found that excessive catalyst dosage leads to inefficient stirring and mixing, resulting in catalyst accumulation, increased mass transfer resistance and hindered TA formation. Consequently, the ideal dosage catalyst for glycerol acetylation over 15SA is 0.5 g, as it achieves the maximum TA selectivity of 55 %.

Effect of Time in Glycerol Acetylation

The effect of reaction time on TA selectivity was investigated by varying the duration from 1 h to 5 h while keeping the other parameters constant at 130 °C, a 1:6 w/v Gly: Ac molar ratio, and 0.5 g of 15SA catalyst, as shown in Figure 12. GLC increased steadily from 97 % to approximately 100 % as the reaction time increased from 1 h to 3 h.

Figure 12 also shows that the TA selectivity rose from 35 % at 1 h to 55 % at 2 h, reaching its maximum at this point, indicating that the reaction achieves its optimal selectivity equilibrium at 2 h. The temporal evolution of acetin selectivity directly reflects the kinetics of the stepwise acetylation on the 15SA surface. In the first hour, the strong acid sites of 15SA rapidly activate acetic acid into acylium ions and drive the initial acetylation of glycerol to produce MA, which constitutes most of the product at t = 1 h. The relatively low TA accumulation at 1 h (35 %) indicates that the MA to DA and DA to TA steps, being less thermodynamically favourable and requiring repeated substrate-surface interaction, have not yet reached completion. This demonstrates that the acetylation of glycerol proceeds

in a stepwise manner, consistent with the findings of Abida et al. (2020) and Mou et al. (2021), who reported that TA selectivity increases progressively with reaction time as MA and DA are sequentially converted through further acetylation with excess acetic acid.

The peak in TA selectivity at 2 h represents the kinetic optimum for this catalyst-substrate system. By this stage, most MA and DA intermediates have been further acetylated on the strong Lewis and Brønsted acid of 15SA, and the reaction has not yet entered the deactivation phase. Notably, the 2 h optimum is shorter than the reported for the catalyst with lower acid strength, which is a direct result of the exclusively strong acid site character of 15SA (T_{max} = 608 °C). This accelerates the rate-limiting third acetylation step and brings the reaction to its selectivity maximum earlier than a catalyst relying on weak or moderate acid sites.

Figure 12 further shows that GLC decreased slightly to 98 % and TA selectivity dropped to 34 % when the reaction was extended to 5 h. This is attributed to the progressive deactivation of the 15SA catalyst at longer reaction times. Water is produced as a by-product of each esterification step, with three moles generated per mole of TA formed. Over-extended reaction times, this accumulated water promotes the hydrolysis of the Ti^{4+}–SO_4^{2-} bond, consistent with the XPS-confirmed Ti-O-S bonding at 530.8 eV, which is susceptible to nucleophilic attack by water. This progressively converts coordinated sulfate species into free sulfuric acid and reduces the density of strong Lewis acid sites (Kale et al., 2015; Shi & Li, 2014). This resulting loss of Lewis activity shifts the product distribution back towards DA and MA, which require less acidic activation. This interpretation aligns with the reusability data in Section 6, where EDX analysis shows the sulfur content declining from 6 % in the fresh catalyst to 2 % in the spent catalyst after five cycles, confirming progressive sulfate leaching as a time- and water- dependent phenomenon. Overall, the optimal reaction time for the 15SA catalyst is 2 h, yielding the highest TA selectivity of 55 % TA alongside 41 % DA, 3 % MA and 97 % GLC.

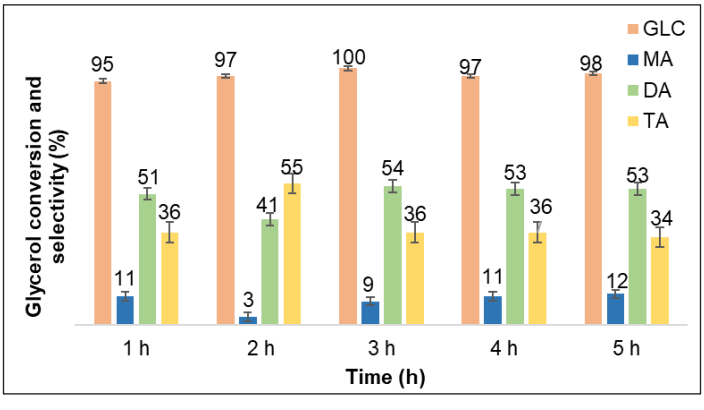

Figure 12. The effect of reaction duration (t) on the GLC and acetins selectivity. (Reaction condition: MR = 1:6 w/v Gly:Ac, CL = 0.5 g, T = 130 °C and t = 1-5 h)

Holistic Mechanistic Interpretation of the Optimal TA selectivity

The four reaction parameters investigated in this study are not independent in their influence on TA selectivity; rather, they interact through a common mechanistic framework governed by the unique physicochemical properties of the 15SA catalyst. The results obtained in Sections 5.1 to 5.4 collectively demonstrate that the peak TA selectivity of 55 % observed at 130 °C, 1:6 w/v Gly: Ac, 0.5 g catalyst loading, and 2 h reaction time arises from the concurrence of several catalyst-specific factors discussed below.

The 15SA catalyst possesses exclusively strong acid sites resulting from the electron-withdrawing effect of SO_4^{2-} groups coordinated to Ti^{4+} centres in the Ti–O–S framework, as confirmed by XPS (O 1s at 530.8 eV; S 2p at 169.4–170.6 eV) and NH_3-TPD (T_{max} = 608 °C, total acidity = 342.6 μmol g^{-1}). The strong Lewis acid sites (Ti^{4+}) activate the carbonyl group of acetic acid into electrophilic acylium ions, while adjacent Brønsted acid sites (Ti–OH, O 1s at 533.9 eV) facilitate the nucleophilic attack of glycerol's hydroxyl groups. The cooperative action of both Lewis and Brønsted acidity on the same catalyst surface enables the full three-step sequential acetylation to proceed to TA under relatively mild conditions, particularly at the moderate temperature of 130 °C.

The optimal temperature of 130 °C is not coincidental. It represents the minimum temperature at which the endothermic DA to TA step proceeds at a rate sufficient to accumulate TA within the 2 h reaction window, while remaining below the threshold at which acetic acid volatilisation under reflux conditions significantly depletes the reagent supply. The mesoporous structure of 15SA (pore diameter 5.2 nm, Type IV isotherm) supports this by accommodating glycerol intermediates (∼1 nm) within the pore channels, enabling multiple sequential encounters with active sites without requiring diffusion to a new particle surface.

The optimal molar ratio of 1:6 w/v ensures that acetic acid is present in sufficient two-fold stoichiometric excess to sustain continuous generation of acylium ions on the strong acid sites, while not overwhelming the limited active site population constrained by the relatively low BET surface area of 15SA (1.9 m^2 g^{-1}) with non-productive competitive adsorption. The optimal catalyst loading of 0.5 g represents the threshold at which the cumulative strong acid site density is sufficient to drive the DA → TA step at 130 °C within 2 h, without triggering agglomeration-induced mass transfer limitations that emerge at higher loadings, as supported by the SEM-observed particle morphology.

Finally, the 2 h reaction time is the kinetic window during which all these conditions converge to achieve maximum TA selectivity. It is sufficiently long for the sequential MA to DA to TA cascade to run to near-completion on the strong acid sites of 15SA, yet short enough to avoid the onset of water-mediated hydrolysis of Ti–O–S bonds that progressively deactivates the catalyst. In summary, the optimal condition yielding 55% TA selectivity and 97% GLC emerges from the concurrence of four factors: sufficient thermal energy to

drive the endothermic TA-forming step, adequate acetic acid excess to sustain acylium ion generation, the right active site density for complete three-step acetylation, and a reaction duration that maximises TA accumulation before catalyst deactivation commences. This finding demonstrates that the physicochemical properties of the 15SA catalyst, specifically its strong acid site density, cooperative Lewis–Brønsted acidity, and mesoporous structure, collectively govern the optimal parametric window for selective TA production in glycerol acetylation.

Reusability Study

The inactivation of the catalytically active sites commonly hampers the industrial application of solid catalysts. Therefore, the stability and deactivation of the 15SA catalyst were determined by studying successive reuse cycles. The reusability study over the 15SA catalyst was investigated under optimal reaction conditions of a molar ratio of 1:6 w/v of Gly: Ac, catalyst dosage of 0.5 g, reaction temperature of 130 °C, for a reaction duration of 2 h.

Figure 13 shows a slight reduction in the selectivity of TA, which decreased from 55 % in the first cycle to 24 % in the fifth cycle, whereas the selectivity of MA and DA increased over the same period. Particularly, in the first cycle, MA and DA had selectivity of 5 % and 41 %, respectively, while in the fifth cycle, MA selectivity increased to 15 % and DA selectivity rose to 61 %. Furthermore, the EDX results shown in Figure 8 revealed that the sulfur content in the fresh catalyst was 6 %, while the sulfur content decreased to 2 % in the spent catalyst as shown in Figure 14. Thus, it is proven that the catalytic activities and the EDX results are aligned with those of Mou et al., (2021), who suggested that the minor reduction in TA selectivity might be due to the loss of the acidity of the catalysts caused by intense stirring, separation, and washing throughout the reaction and recovery process. Additionally, it is advised that additional investigation be conducted using XPS and TGA analysis to further confirm whether the sulfate species were leached out from the 15SA catalyst or experienced structural changes following its use in the reaction. Fortunately, the DA selectivity in this study remains high at 61 % after five cycles, indicating that the leaching of the active sites only inhibits the diffusion of TA molecules on the catalyst surface, resulting in lower TA selectivity. This finding is aligned with Testa et al., (2019).

Moreover, it is clearly seen in Figure 13 that the conversion of glycerol (GLC) from the first cycle to the second cycle slightly improved from 97 % to 100 % and remained excellent after being reutilised for five cycles. This discovery suggests that the further leaching of sulfate species from the catalyst's surface may result in a larger surface area of the catalyst, thereby improving the conversion of the glycerol. This observation aligned with the BET results in Table 1, where the non-sulfated titania exhibited a larger BET surface area of 11. 8 m^2g^{-1} while 15SA exhibited a BET surface area of 1.9 m^2g^{-1}.

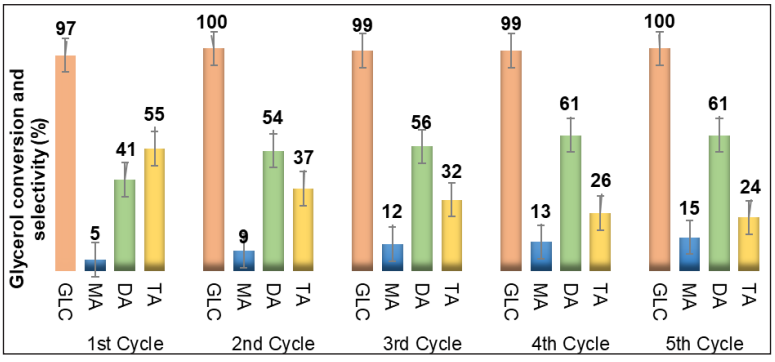

Figure 13. Reusability study using sulfated-titania catalyst (15SA). (Reaction condition: MR = 1:6 w/v Gly:Ac, CL = 0.5 g, t = 2 h and T = 130 °C)

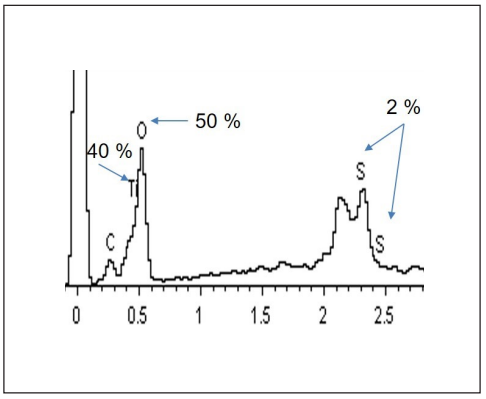

Figure 14. EDX result for the spent 15SA catalyst

Therefore, this discovery suggests that apart from having sufficient BET surface area, the catalyst used in the glycerol acetylation requires strong acidic sites to push forward the reaction toward higher TA selectivity. Furthermore, Herrada-Vidales et al. (2020) state that the mixture of DA and TA can also be utilised as a fuel additive due to their comparable properties, such as high hydrocarbon solubility, low water affinity, and high additive effect. Therefore, DA and TA do not need to be separated before their use in biodiesel and gasoline. As oxygenated fuel additives, a mixture of DA and TA could also diminish the emission of toxic gases and the number of particles in the exhaust fume and provide better combustion in the cylinder (Malaika et al., 2023). Therefore, Figure 13 shows that the utilisation of the 15SA catalyst at optimal conditions exhibits a higher mixture of DA and TA selectivity, exceeding 85 %. This result indicates that the 15SA catalyst has a great deal to produce fuel additives by acetylation under mild reaction conditions. Additionally, the reusability study over the 15SA catalyst concluded that the leaching of the sulfate species from the solid catalyst is an unavoidable phenomenon that caused lower TA selectivity in subsequent uses in the reaction. Therefore, it is recommended to conduct further studies to investigate suitable methods and solvents used for regenerating the catalyst before its use in the next reaction to minimise sulfate species leaching while maintaining high TA selectivity until five complete cycles.

CONCLUSION

The sulfated-titania catalyst (15SA) was prepared using the impregnation method with a 15% sulfuric acid concentration. The catalyst was successfully evaluated in the parametric study to observe the influence of temperature, loading of the catalyst, molar ratio of Gly: Ac and reaction time on glycerol conversion and acetins selectivity. The robust acidic strength, sufficient BET surface area and good porosity of the 15SA catalyst facilitate a higher TA selectivity of 55 % at optimal conditions of a 1:6 w/v Gly: Ac molar ratio, utilising a catalyst dosage of 0.5 g at a reaction temperature of 130 °C for a 2 h reaction. In the reusability study, the 15SA catalyst was successfully utilised in the fifth consecutive cycle, achieving excellent GLC over 97%. In contrast, the selectivity of TA dropped from 55 % to 24 % for the first to the fifth cycles, respectively. Fortunately, the DA selectivity remained high, achieving 61 % and DA+TA selectivity, exceeding 85 % throughout five cycles. This observation indicates that the 15SA catalyst can generate more fuel additives consisting of a mixture of DA and TA, thereby potentially replacing homogenous catalysts that have difficulties in separation, are highly toxic and cannot be reused or regenerated. It is also acknowledged that the one-factor-at-a-time (OFAT) approach used in this study does not account for potential interaction effects between reaction parameters such as temperature, molar ratio, catalyst loading, and reaction time. For future work, it is recommended to employ multivariate statistical design methods, such as Response Surface Methodology (RSM) or Central Composite Design (CCD), to comprehensively evaluate parameter interactions and validate the optimal conditions identified in this study.

Declaration of Competing Interest

The authors declare no known competing financial interests or personal relationships that could have appeared to influence this work.

ACKNOWLEDGEMENT

The authors deeply appreciate the GPPI grant (GPPI/2019/9676400) from Universiti Putra Malaysia, and UTM-UPM CRG (Matching Grant/2019/9300458). Catalysis Science and Technology Research Centre (PutraCat) is also gratefully acknowledged.

REFERENCES

Abida, K., Chudasama, B., & Ali, A. (2020). Development and functionalisation of magnetic nanoparticles as stable and reusable catalysts for triacetin synthesis. *New Journal of Chemistry, 44*(22), 9365-9376. https://doi.org/10.1039/D0NJ00488J

Afshar, S., Sadehvand, M., Azad, A., Dekamin, M. G., Jalali-Heravi, M., Mollahosseini, A., Amani, M., & Tadjarodi, A. (2015). Optimisation of catalytic activity of sulfated titania for efficient synthesis of isoamyl

acetate by response surface methodology. *Monatshefte für Chemie – Chemical Monthly, 146*(12), 1949-1957. https://doi.org/10.1007/s00706-015-1533-5

Appaturi, J. N., Maireles-Torres, P., Alomar, T. S., Najla, A., El-Bahy, Z. M., Ling, T. C., & Ng, E. P. (2023). Highly active nickel (II) oxide-supported cerium oxide fuel additives. *Materials, 16*(13), Article 4713. https://doi.org/10.3390/ma16134713

Appaturi, J. N., Ramalingam, R. J., Selvaraj, M., Chia, S., Tan, S. H., Khoerunnisa, F., Ling, T. C., & Ng, E. P. (2021). Selective synthesis of triacetyl glyceride biofuel additive via acetylation of glycerol over NiO-supported TiO_2 catalyst enhanced by non-microwave instant heating. *Applied Surface Science, 545*, Article 149017. https://doi.org/10.1016/j.apsusc.2021.149017

Azri, N., Irmawati, R., Nda-Umar, U. I., Saiman, M. I., & Taufiq-Yap, Y. H. (2021). Promotional effect of transition metals (Cu, Ni, Co, Fe, Zn)-supported on dolomite for hydrogenolysis of glycerol into 1,2-propanediol. *Arabian Journal of Chemistry, 14*(4), Article 103047. https://doi.org/10.1016/j.arabjc.2021.103047

Beejapur, H. A., La Parola, V., Liotta, L. F., & Testa, M. L. (2017). Glycerol acetylation over organic–inorganic sulfonic or phosphonic silica catalysts. *ChemistrySelect, 2*(17), 4934-4941. https://doi.org/10.1002/slct.201700934

Carpegiani, J. A., Godoy, W. M., Guimarães, D. H. P., & Aguiar, L. G. (2020). Glycerol acetylation catalysed by an acidic styrene-co-dimethacrylate resin: Experiments and kinetic modelling. *Reaction Kinetics, Mechanisms and Catalysis, 130*(1), 447-461. https://doi.org/10.1007/s11144-020-01788-7

Chandrakala, U., Prasad, R. B. N., & Prabhavathi Devi, B. L. A. (2014). Glycerol valorisation as biofuel additives by employing a carbon-based solid acid catalyst derived from glycerol. *Industrial & Engineering Chemistry Research, 53*(42), 16164-16169. https://doi.org/10.1021/ie503079m

Chilakamarry, C. R., Sakinah, A. M. M., Zularisam, A. W., & Pandey, A. (2021). Glycerol waste to value-added products and its potential applications. *Systems Microbiology and Biomanufacturing, 1*(4), 378-396. https://doi.org/10.1007/s43393-021-00036-w

da Silva, D. S., Altino, F. M. R. S., Bortoluzzi, J. H., & Meneghetti, S. M. P. (2020). Investigation of Sn(IV) catalysts in glycerol acetylation. *Molecular Catalysis, 494*, Article 111130. https://doi.org/10.1016/j.mcat.2020.111130

Dabbawala, A. A., Alhassan, S. M., Mishra, D. K., Jegal, J., & Hwang, J. S. (2018). Solvent-free cyclodehydration of sorbitol to isosorbide over mesoporous sulfated titania with enhanced catalytic performance. *Molecular Catalysis, 454*, 77-86. https://doi.org/10.1016/j.mcat.2018.05.009

Dalla Costa, B. O., Decolatti, H. P., Legnoverde, M. S., & Querini, C. A. (2017). Influence of acidic properties of different solid acid catalysts for glycerol acetylation. *Catalysis Today, 289*, 222-230. https://doi.org/10.1016/j.cattod.2016.09.015

Dantas, J., Leal, E., Mapossa, A. B., Cornejo, D. R., & Costa, A. C. F. M. (2017). Magnetic nanocatalysts of Ni0.5Zn0.5Fe2O4 doped with Cu and performance evaluation in transesterification reaction for biodiesel production. *Fuel, 191*, 463-471. https://doi.org/10.1016/j.fuel.2016.11.107

Dey, S., Reang, N. M., Das, P. K., & Deb, M. (2021). A comprehensive study on the prospects of the economy, environment, and efficiency of palm oil biodiesel as a renewable fuel. *Journal of Cleaner Production, 286*, Article 124981. https://doi.org/10.1016/j.jclepro.2020.124981

Dhawan, M. S., Barton, S. C., & Yadav, G. D. (2021). Interesterification of triglycerides with methyl acetate for the co-production of biodiesel and triacetin using hydrotalcite as a heterogeneous base catalyst. *Catalysis Today, 375*, 101-111. https://doi.org/10.1016/j.cattod.2020.07.056

Ebadi Pour, N., Dumeignil, F., Katryniok, B., Delevoye, L., Revel, B., & Paul, S. (2021). Investigating the active phase of Ca-based glycerol polymerisation catalysts: On the importance of calcium glycerolate. *Molecular Catalysis, 507*, Article 111571. https://doi.org/10.1016/j.mcat.2021.111571

Enríquez, J. M. H., Lajas, L. A. C., Alamilla, R. G., Martín, E. Á. S., Alamilla, G. P., Handy, E. B., Galindo, G. C., & Serrano, L. A. G. (2013). Synthesis of solid acid catalysts based on TiO_2–SO_4 applied in *n*-hexane isomerisation. *Journal of Metal, 3*(3), 34-44.

Fauzi, M., Termezi, A., Izyanni, S., Hizami, M., & Yusoff, M. (2025). Effect of Fe and Ni loading in Fe–Ni supported on activated carbon catalyst on glycerol acetylation to acetins. *Sustainable Chemistry for the Environment, 10*, Article 100162. https://doi.org/10.1016/j.scenv.2025.100162

Ferreira, P., Fonseca, I. M., Ramos, A. M., Vital, J., & Castanheiro, J. E. (2009). Esterification of glycerol with acetic acid over dodecamolybdophosphoric acid encaged in USY zeolite. *Catalysis Communications, 10*(5), 481-484. https://doi.org/10.1016/j.catcom.2008.10.015

Fronza, C. S., Nunes, A. L. B., Castilhos, F., & Salau, N. P. G. (2025). Niobium-based catalysts for glycerol valorisation via acetylation: A sustainable path to fuel additives. *Energy Conversion and Management, 342*, Article 120146. https://doi.org/10.1016/j.enconman.2025.120146

García-Martín, J. F., Alés-Álvarez, F. J., Torres-García, M., Feng, C. H., & Álvarez-Mateos, P. (2019). Production of oxygenated fuel additives from residual glycerine using biocatalysts obtained from heavy-metal-contaminated *Jatropha curcas* L. roots. *Energies, 12*(4), Article 740. https://doi.org/10.3390/en12040740

Gardy, J., Hassanpour, A., Lai, X., & Ahmed, M. H. (2016). Synthesis of $Ti(SO_4)O$ solid acid nano-catalyst and its application for biodiesel production from used cooking oil. *Applied Catalysis A: General, 527*, 81-95. https://doi.org/10.1016/j.apcata.2016.08.031

Geetha, S., Thangamani, A., Valliappan, R., Vedanayaki, S., & Ganapathi, A. (2020). Sulfated titania (TiO_2-SO_4^{2-}) as an efficient and reusable solid acid catalyst for the multi-component synthesis of highly functionalised piperidines. *Chemical Data Collections, 30*, Article 100565. https://doi.org/10.1016/j.cdc.2020.100565

Herrada-Vidales, J. A., García-González, J. M., Martínez-Palou, R., & Guzmán-Pantoja, J. (2020). Integral process for obtaining acetins from crude glycerol and their effect on the octane index. *Chemical Engineering Communications, 207*(2), 231-241. https://doi.org/10.1080/00986445.2019.1578758

Hidayati, N., Khoiruddin, W., Purnama, H., & Effendy, M. (2024a). Synthesis and characterisation of graphene oxide catalysts for glycerol acetylation. *Bulletin of Chemical Reaction Engineering and Catalysis, 19*(2), 340-349. https://doi.org/10.9767/bcrec.20146

Hidayati, N., Rahma Maulida, I., Purnama, H., Musthofa, M., & Ur Rahmah, A. (2024b). Optimisation of the glycerol acetylation process using graphene oxide catalyst. *South African Journal of Chemical Engineering, 48*, 254-264. https://doi.org/10.1016/j.sajce.2024.02.011

Hu, W., Zhang, Y., Huang, Y., Wang, J., Gao, J., & Xu, J. (2015). Selective esterification of glycerol with acetic acid to diacetin using antimony pentoxide as reusable catalyst. *Journal of Energy Chemistry, 24*(5), 632-636. https://doi.org/10.1016/j.jechem.2015.08.001

Huang, Z., Lin, Y., Li, L., Ye, C., & Qiu, T. (2017). Preparation and shaping of solid acid SO_4^{2-}/TiO_2 and its application for esterification of propylene glycol monomethyl ether and acetic acid. *Chinese Journal of Chemical Engineering, 25*(9), 1207-1216. https://doi.org/10.1016/j.cjche.2016.11.006

Jenie, S. N. A., Kusuma, D. S., Kristiani, A., Laksmono, J. A., & Tursiloadi, S. (2010). Preparation and characterisation of sulfated titania catalysts for the isomerisation of citronellal. *International Journal of Basic and Applied Science, 10*(06), 5-10.

Jiang, Y., Li, X., Zhao, H., & Hou, Z. (2019). Esterification of glycerol with acetic acid over SO_3H-functionalized phenolic resin. *Fuel, 255*, Article 115842. https://doi.org/10.1016/j.fuel.2019.115842

Jose, M., Paloma, N., Lopes, G., & Rodrigues, A. A. (2023). Biodiesel additives synthesis using solid heteropolyacid catalysts. *Energies, 16*(3), Article 1332. https://doi.org/10.3390/en16031332

Kale, S., Umbarkar, S. B., Dongare, M. K., Eckelt, R., Armbruster, U., & Martin, A. (2015). Selective formation of triacetin by glycerol acetylation using acidic ion-exchange resins as a catalyst and toluene as an entrainer. *Applied Catalysis A: General, 490*, 10-16. https://doi.org/10.1016/j.apcata.2014.10.059

Kalyani, T., Prasad, L. S. V., & Kolakoti, A. (2023). Effect of triacetin as an oxygenated additive in algae biodiesel fuelled CI engine combustion, performance, and exhaust emission analysis. *Fuel, 338*, Article 127366. https://doi.org/10.1016/j.fuel.2022.127366

Kanimozhi, S., Ramani, V., & Pandurangan, A. (2018). Effects of alumina on GO and KIT-6 supports for the acetylation of glycerol. *New Journal of Chemistry, 42*(18), 15197-15208. https://doi.org/10.1039/C8NJ01833B

Karnjanakom, S., Maneechakr, P., Samart, C., & Guan, G. (2018). Ultrasound-assisted acetylation of glycerol for triacetin production over green catalyst: A liquid biofuel candidate. *Energy Conversion and Management, 173*, 262-270. https://doi.org/10.1016/j.enconman.2018.07.086

Khayoon, M. S., Triwahyono, S., Hameed, B. H., & Jalil, A. A. (2014). Improved production of fuel oxygenates via glycerol acetylation with acetic acid. *Chemical Engineering Journal, 243*, 473-484. https://doi.org/10.1016/j.cej.2014.01.027

Kulkarni, R. M., Britto, P. J., Narula, A., Saqline, S., Anand, D., Bhagyalakshmi, C., & Herle, R. N. (2020). Kinetic studies on the synthesis of fuel additives from glycerol using CeO_2–ZrO_2 metal oxide catalyst. *Biofuel Research Journal, 7*(1), 1100-1108. https://doi.org/10.18331/BRJ2020.7.1.2

Ladero, M. (2021). New glycerol upgrading processes. *Catalysts, 11*(1), Article 103. https://doi.org/10.3390/catal11010103

Lee, Y., Kao, Y., Xu, H., Tsunekawa, S., & Yoshida, M. (2026). Green synthesis of glycerol carbonate from glycerol and CO_2 using a polymeric ionic liquid catalyst: An experimental and theoretical study. *Journal of Cleaner Production, 560*, Article 148344. https://doi.org/10.1016/j.jclepro.2026.148344

Lertna, N., Srisamut, P., Supapan, N., Athikaphan, P., Rood, S. C., Neramittagapong, A., & Neramittagapong, S. (2022). Synthesis of sulfated titanium dioxide catalyst for sorbitol dehydration to isosorbide. *Materials Today: Proceedings, 75*, 91-98. https://doi.org/10.1016/j.matpr.2022.11.226

Liu, G., Tsen, W. C., Hu, F., Zhong, F., Wang, J., Liu, H., Wen, S., Zheng, G., Qin, C., & Gong, C. (2020). Enhanced proton conductivities of chitosan-based membranes by inorganic solid superacid SO_4^{2-}–TiO_2 coated carbon nanotubes. *International Journal of Hydrogen Energy, 45*(53), 29212-29221. https://doi.org/10.1016/j.ijhydene.2020.07.157

Liu, J., Wang, Z., Sun, Y., Jian, R., Jian, P., & Wang, D. (2019). Selective synthesis of triacetin from glycerol catalysed by HZSM-5/MCM-41 micro/mesoporous molecular sieve. *Chinese Journal of Chemical Engineering, 27*(5), 1073-1078. https://doi.org/10.1016/j.cjche.2018.09.013

Magar, S., Mohanraj, G. T., Jana, S. K., & Rode, C. V. (2020). Synthesis and characterisation of supported heteropoly acid: Efficient solid acid catalyst for glycerol esterification to produce biofuel additives. *Inorganic and Nano-Metal Chemistry, 50*(11), 1157-1165. https://doi.org/10.1080/24701556.2020.1737817

Malaika, A., Mesjasz, D., & Kozłowski, M. (2023). Maximising the selectivity to triacetin in glycerol acetylation through a plastic waste-derived carbon catalyst development and selection of a reaction unit. *Fuel, 333*, Article 126271. https://doi.org/10.1016/j.fuel.2022.126271

Mou, R., Wang, X., Wang, Z., Zhang, D., Yin, Z., Lv, Y., & Wei, Z. (2021). Synthesis of fuel bioadditive by esterification of glycerol with acetic acid over hydrophobic polymer-based solid acid. *Fuel, 302*, Article 121175. https://doi.org/10.1016/j.fuel.2021.121175

Mufrodi, Z., Rochmadi, Sutijan, & Budiman, A. (2014). Synthesis of acetylation of glycerol using a batch reactor and a continuous reactive distillation column. *Engineering Journal, 18*(2), 29-39. https://doi.org/10.4186/ej.2014.18.2.29

Mukhopadhyay, P., Chakraborty, R., & Singh, S. (2021). Triacetin additive in biodiesel to reduce air pollution: A review. *Environmental Chemistry Letters, 20*(1), 3-27. https://doi.org/10.1007/s10311-021-01362-0

Nda-Umar, U. I., Irmawati, R., Muhamad, E. N., Azri, N., & Taufiq-Yap, Y. H. (2020a). Optimisation and characterisation of mesoporous sulfonated carbon catalyst and its application in modelling and optimisation of acetin production. *Molecules, 25*(22), Article 5221. https://doi.org/10.3390/molecules25225221

Nda-Umar, U. I., Irmawati, R., Muhamad, E. N., Taufiq-Yap, Y. H., & Azri, N. (2020b). Synthesis and characterisation of sulfonated carbon catalysts derived from biomass waste and their evaluation in glycerol acetylation. *Biomass Conversion and Biorefinery, 12*, 1143-1158. https://doi.org/10.1007/s13399-020-00784-0

Neto, A. B. S., Oliveira, A. C., Rodriguez-Castellón, E., Campos, A. F., Freire, P. T. C., Sousa, F. F. F., Filho, J. M., Araujo, J. C. S., & Lang, R. (2020). A comparative study on porous solid acid oxides as catalysts in the esterification of glycerol with acetic acid. *Catalysis Today, 349*, 57-67. https://doi.org/10.1016/j.cattod.2018.05.057

Noda, L. K., de Almeida, R. M., Gonçalves, N. S., Probst, L. F. D., & Sala, O. (2003). TiO_2 with a high sulfate content: Thermogravimetric analysis, determination of acid sites by infrared spectroscopy and catalytic activity. *Catalysis Today, 85*(1), 69-74. https://doi.org/10.1016/S0920-5861(03)00195-0

Okoye, P. U., Abdullah, A. Z., & Hameed, B. H. (2017a). A review on recent developments and progress in the kinetics and deactivation of catalytic acetylation of glycerol—A byproduct of biodiesel. *Renewable and Sustainable Energy Reviews, 74*, 387-401. https://doi.org/10.1016/j.rser.2017.02.017

Okoye, P. U., Abdullah, A. Z., & Hameed, B. H. (2017b). Synthesis of oxygenated fuel additives via glycerol esterification with acetic acid over bio-derived carbon catalyst. *Fuel, 209*, 538-544. https://doi.org/10.1016/j.fuel.2017.08.024

Okoye, P. U., & Hameed, B. H. (2016). Review of recent progress in catalytic carboxylation and acetylation of glycerol as a byproduct of biodiesel production. *Renewable and Sustainable Energy Reviews, 53*, 558-574. https://doi.org/10.1016/j.rser.2015.08.064

Parida, K. M., Sahu, N., Biswal, N. R., Naik, B., & Pradhan, A. C. (2008). Preparation, characterisation, and photocatalytic activity of sulfate-modified titania for degradation of methyl orange under visible light. *Journal of Colloid and Interface Science, 318*(2), 231-237. https://doi.org/10.1016/j.jcis.2007.10.028

Patil, S. M., Deshmukh, S. P., More, K. V., Shevale, V. B., Mullani, S. B., Dhodamani, A. G., & Delekar, S. D. (2019). Sulfated TiO_2/WO_3 nanocomposite: An efficient photocatalyst for degradation of Congo red and methyl red dyes under visible light irradiation. *Materials Chemistry and Physics, 225*, 247-255. https://doi.org/10.1016/j.matchemphys.2018.12.041

Pratika, R. A., Wijaya, K., & Trisunaryanti, W. (2021). Hydrothermal treatment of SO_4/TiO_2 and TiO_2/CaO as heterogeneous catalysts for the conversion of Jatropha oil into biodiesel. *Journal of Environmental Chemical Engineering, 9*(6), Article 106547. https://doi.org/10.1016/j.jece.2021.106547

Pratika, R. A., Wijaya, K., Utami, M., Mulijani, S., Patah, A., Alarifi, S., Ram Mani, R., Kumar Yadav, K., Ravindran, B., Chung, W. J., Chang, S. W., & Munusamy-Ramanujam, G. (2023). The potency of hydrothermally prepared sulfated silica (SO_4/SiO_2) as a heterogeneous acid catalyst for ethanol dehydration into diethyl ether. *Chemosphere, 341*, Article 139822. https://doi.org/10.1016/j.chemosphere.2023.139822

Ramos, L. D., Ramírez, A. E., & Miranda, C. D. (2025). Acidic eco-catalysts derived from coffee husks in the acetylation of glycerol. *Tetrahedron Green Chemistry, 5*, Article 100075. https://doi.org/10.1016/j.tgchem.2025.100075

Rathod, S., Joshi, K. K., Patel, D., Pataniya, P., Nandpal, M. N., Patel, S. G., Sumesh, C. K., & Kapatel, S. (2025). Facile surface reconstructions of cobalt–copper oxide heterostructures enable efficient electrocatalytic glycerol oxidation for energy-saving hydrogen evolution. *Journal of Alloys and Compounds, 1048*, Article 185267. https://doi.org/10.1016/j.jallcom.2025.185267

Reddy, P. S., Sudarsanam, P., Raju, G., & Reddy, B. M. (2010). Synthesis of bio-additives: Acetylation of glycerol over zirconia-based solid acid catalysts. *Catalysis Communications, 12*(1), 62-65. https://doi.org/10.1016/j.catcom.2010.07.006

Reinoso, D. M., & Boldrini, D. E. (2020). Kinetic study of fuel bio-additive synthesis from glycerol esterification with acetic acid over acid polymeric resin as a catalyst. *Fuel, 264*, Article 116879. https://doi.org/10.1016/j.fuel.2019.116879

Ropero-Vega, J. L., Aldana-Pérez, A., Gómez, R., & Niño-Gómez, M. E. (2010). Sulfated titania (TiO_2/SO_4^{2-}): A very active solid acid catalyst for the esterification of free fatty acids with ethanol. *Applied Catalysis A: General, 379*(1-2), 24-29. https://doi.org/10.1016/j.apcata.2010.02.020

Shera Farisya, M. R., Irmawati, R., Shafizah, I. N., Taufiq-Yap, Y. H., Muhamad, E. N., Lee, S. L., & Salamun, N. (2021). Assessment of the effect of sulfuric acid concentration on physicochemical properties of sulfated-titania catalyst and glycerol acetylation performance. *Catalysts, 11*(12), Article 1542. https://doi.org/10.3390/catal11121542

Shi, W., & Li, J. (2014). A deactivation mechanism of sulfated titania in the esterification of acetic acid and *n*-butanol. *Reaction Kinetics, Mechanisms and Catalysis, 111*(1), 215-233. https://doi.org/10.1007/s11144-013-0628-4

Shikhaliyev, K., Hameed, B. H., & Okoye, P. U. (2021). Utilisation of biochars as sustainable catalysts for the upgrading of glycerol from biodiesel production. *Journal of Environmental Chemical Engineering, 9*(2), Article 104768. https://doi.org/10.1016/j.jece.2020.104768

Silva, L. N., Gonçalves, V. L. C., & Mota, C. J. A. (2010). Catalytic acetylation of glycerol with acetic anhydride. *Catalysis Communications, 11*(12), 1036-1039. https://doi.org/10.1016/j.catcom.2010.05.007

Singh, R. K., & Gosu, V. (2025). Catalytic acetalization of glycerol to solketal using mesoporous silica. *Applied Catalysis A: General, 703*, Article 120350. https://doi.org/10.1016/j.apcata.2025.120350

Spataru, D., Soares Dias, A. P., & Vieira Ferreira, L. F. (2021). Acetylation of biodiesel glycerin using glycerin and glucose-derived catalysts. *Journal of Cleaner Production, 297*, Article 126686. https://doi.org/10.1016/j.jclepro.2021.126686

Srivastava, S., Jadeja, G. C., & Parikh, J. (2017). Synergism studies on alumina-supported copper-nickel catalysts towards furfural and 5-hydroxymethylfurfural hydrogenation. *Journal of Molecular Catalysis A: Chemical, 426*, 244-256. https://doi.org/10.1016/j.molcata.2016.11.023

Testa, M. L., La Parola, V., Mesrar, F., Ouanji, F., Kacimi, M., Ziyad, M., & Liotta, L. F. (2019). Use of zirconium phosphate-sulphate as an acid catalyst for the synthesis of glycerol-based fuel additives. *Catalysts, 9*(2), Article 148. https://doi.org/10.3390/catal9020148

Timofeeva, M. N., Panchenko, V. N., Khan, N. A., Hasan, Z., Prosvirin, I. P., Tsybulya, S. V., & Jhung, S. H. (2017). Isostructural metal-carboxylates MIL-100(M) and MIL-53(M) (M: V, Al, Fe and Cr) as catalysts for the condensation of glycerol with acetone. *Applied Catalysis A: General, 529*, 167-174. https://doi.org/10.1016/j.apcata.2016.11.006

Tomer, R., & Biswas, P. (2020). Dehydration of glucose/fructose to 5-hydroxymethylfurfural (5-HMF) over an easily recyclable sulfated titania (SO_4^{2-}/TiO_2) catalyst. *New Journal of Chemistry, 44*(47), 20734-20750. https://doi.org/10.1039/D0NJ04151C

Wang, J., Pan, H., Wang, A., Tian, X., Wu, X., & Wang, Y. (2015). Synthesis and characterisation of $S_2O_8^{2-}/ZnFe_xAl_{2-x}O_4$ solid acid catalysts for the esterification of acetic acid with *n*-butanol. *Catalysis Communications, 62*, 29-33. https://doi.org/10.1016/j.catcom.2015.01.009

Wijaya, K., Putri, A. R., Sudiono, S., Mulijani, S., Patah, A., Wibowo, A. C., & Saputri, W. D. (2021). Effectively synthesizing SO_4/TiO_2 catalyst and its performance for converting ethanol into diethyl ether (DEE). *Catalysts, 11*(12), Article 1492. https://doi.org/10.3390/catal11121492

Yang, W., Ok, Y. S., Dou, X., Zhang, Y., Yang, M., Wei, D., & Xu, P. (2019). Effectively remediating spiramycin from production wastewater through hydrolysis of its functional groups using solid superacid TiO_2/SO_4. *Environmental Research, 175*, 393-401. https://doi.org/10.1016/j.envres.2019.05.037

Zhao, H., Jiang, P., Dong, Y., Huang, M., & Liu, B. (2014). A high-surface-area mesoporous sulfated nano-titania solid superacid catalyst with exposed (101) facets for esterification: Facile preparation and catalytic performance. *New Journal of Chemistry, 38*(9), 4541-4548. https://doi.org/10.1039/C4NJ00494A